Applied Radiation and Isotopes 70 (2012) 1206–1209

Contents lists available at SciVerse ScienceDirect

Applied Radiation and Isotopes

journal homepage: www.elsevier.com/locate/apradiso

Reconstruction of the relief of an investigated object with scanning X-ray fluorescence microanalysis and Monte Carlo simulations of surface effects

T. Trojek*

Department of Dosimetry and Application of Ionizing Radiation, Czech Technical University in Prague, Czech Republic

ARTICLE INFO

Available online 11 November 2011

Keywords:
X-ray fluorescence analysis
Surface effect
Monte Carlo

ABSTRACT

This paper describes surface effects in microscopic X-ray fluorescence analysis, including the Monte Carlo simulations of the production and the detection of characteristic radiation. A new data analysis technique is also introduced. It enables us to make improved calculations of element concentrations and to determine the shape of the surface in an analyzed spot. Finally, reliefs of two scanned objects are presented. Good results were achieved, especially for a metallic object containing chemical elements only measurable with X-ray fluorescence analysis.

1. Introduction

It is well known that the shape of an acquired X-ray spectrum in X-ray fluorescence analysis does not depend solely on the composition of the investigated object. The influence of surface irregularities can also be significant, especially for untreated samples. This disturbing effect, known as the surface effect, makes quantitative analysis less accurate (Rindby et al., 1996, Milazzo and Cicardi, 1997). However, the increase or decrease in X-ray intensities holds information on the surface properties of the analyzed sample. The topography of the surface can be determined in scanning X-ray fluorescence analysis or microanalysis. This study works on suppressing surface effects and determining a relief image of an investigated object using the data from scanning microscopic X-ray fluorescence (μ-XRF) analysis.

Imaging at micro- and nano-scale is widely carried out with a scanning electron microscope (SEM). This image contains information about the surface topography, composition, and other properties such as electrical conductivity (Eberhart, 1995). X-ray imaging based on the emission of characteristic radiation cannot produce very good spatial resolution of SEM. However, its main purpose is to separate topographic and concentration images.

The intensities of X-rays emitted from a sample or detected count rates can nowadays be calculated analytically with formulas based on the Sherman equation, or numerically with the Monte Carlo simulations. Several authors are engaged in modeling X-ray interaction in matter and in producing characteristic radiation (Scot et al., 2007, Hansson and Isaksson, 2007, or Czyzycki et al., 2011). In this work, the MCNPX code (MCNPX User's Manual, 2002) is applied. It can be used in energy dispersive X-ray fluorescence because atomic relaxation processes are implemented, the emission of characteristic radiation is taken into account, and it has been validated by comparing calculated and measured X-ray spectra (Trojek and Wegrzynek, 2010).

2. Theory and Monte Carlo simulations

Surface effects can be easily demonstrated with Monte Carlo calculations, as shown by Trojek et al. (2010). Two dimensional XRF scanning of a sample made of invar alloy (Fe—64%, Ni—36%) was simulated with the MCNPX code. The scanned area ($50\times 26\ \mu m^2$) of the sample is smooth, apart from the presence of the hemisphere with a radius of 10 μm, see Fig. 1. The monoenergetic X-ray beam of energy 17.4 keV (Kα line of molybdenum) and 1 μm in diameter strikes various parts of the surface of the sample and the fluences of characteristic X-rays were calculated in the place of the detector. The incident and emergent angles are 45° and 90°, respectively. The whole area of the sample was split into 25 pixels × 13 pixels with a step of 2 μm, and the fluences of the iron and nickel Kα lines were determined for each of them. If the surface is smooth or the surface effect does not make itself felt, the X-ray fluences should be same for all pixels. However, Fig. 2a and b shows strong fluctuations of X-ray fluences according to local shape of the surface. The position of the hemisphere is indicated by a circle. The fluences are normalized to the response of the smooth surface. It is evident that the presence of the hemisphere decreases or increases the fluences, because it extends or cuts down the mean path length of the characteristic radiation in the sample in the direction towards the detector. Since the radius of the hemisphere is only 10 μm, its

* Tel.: +420 224 358 237; fax: +420 224 811 074.
E-mail address: tomas.trojek@fjfi.cvut.cz

0969-8043/$ - see front matter © 2011 Elsevier Ltd. All rights reserved.
doi:10.1016/j.apradiso.2011.11.012

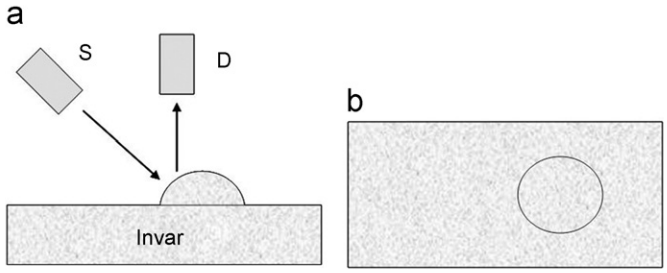

Fig. 1. (a) Simulation of 2D scanning of an invar alloy; the surface roughness is represented by a hemisphere 10 μm in radius; S—X-ray source, D—detector (b) top view.

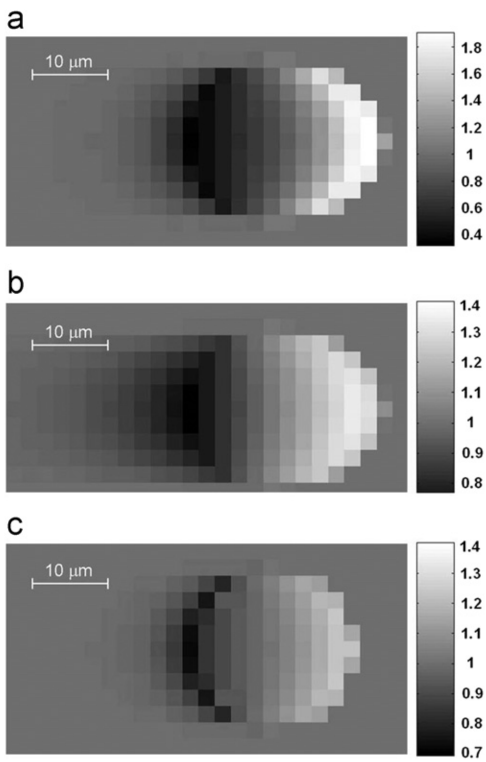

Fig. 2. Relative fluences of characteristic radiation determined with a Monte Carlo simulation of μ-XRF scanning of invar sample. The position of an invar hemisphere on the smooth surface is indicated. (a) Kα line of nickel (geometry 45°/90°); (b) Kα line of iron (geometry 45°/90°); (c) Kα line of iron (geometry 75°/90°).

presence influences the analysis of a much larger area. This is caused by the considerable mean free paths of X-rays in invar alloy. Concretely, they are 30.3 μm for energy 17.4 keV (Kα line of molybdenum), 15.7 μm for 6.4 keV (Kα line of iron), and only 4.9 μm for 7.47 keV (Kα line of nickel). Thanks to the high absorption of nickel X-rays, the "shadow" in Fig. 2a is smaller than it is for the iron X-rays in Fig. 2b.

The calculated relative X-ray fluences in Fig. 2 are consistent with the relative count rates N_i of the characteristic X-rays of element i that would be measured under the same conditions (Trojek, 2007). A selected quantitative XRF analysis method can therefore be applied and the fluences can be converted to element concentrations. The easiest method is a direct comparison between the count rate N_i and the concentration C_i of element i:

$$N_i = K_i C_i \tag{1}$$

where K_i is the instrumental constant for element i, and it must be determined from the X-ray fluence calculated for a smooth surface of the invar alloy. Neither absorption effects nor enhancement effects are taken into consideration. This method provided

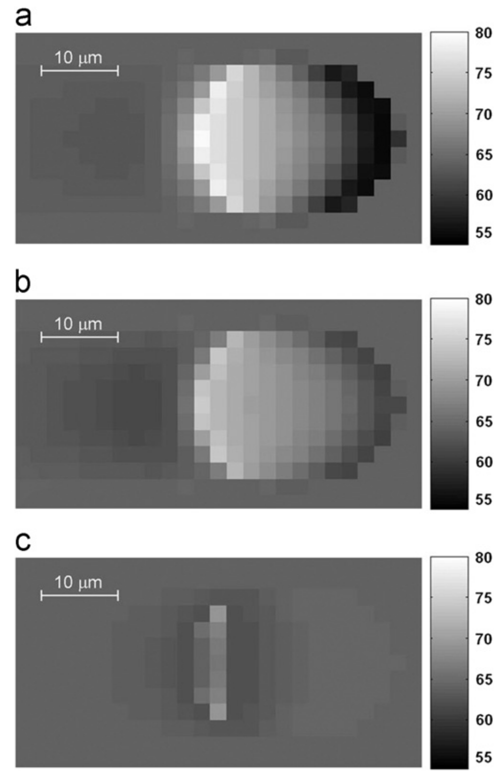

Fig. 3. Iron concentrations [%] in invar sample determined by 3 methods of quantitative analysis for geometry 45°/90°. (a) Method based on direct comparison between count rate and concentration; (b) fundamental parameter method; (c) improved method using parameter θ.

concentrations of iron 44%–85%, and concentrations of nickel from 11% to 69%. These intervals are very wide, and many of the results are far from the correct values. When the sum of the concentration of nickel and iron was normalized to 100%, better results were achieved. However, these results, shown in Fig. 3a, still suffer from high variability.

A more precise result should be obtained using a fundamental parameter method that takes into account differences in the absorption of incident and fluorescence radiation and does not neglect secondary fluorescence radiation. The count rate is given by formula (2):

$$N_i = K_i C_i \left(\frac{\tau_{1,i}/\sin(\varphi_1)}{(\mu_1/\sin(\varphi_1)) + (\mu_2/\sin(\varphi_2))} + \text{Sec. fluorescence} \right) \tag{2}$$

where $\tau_{1,i}$—mass photoelectric attenuation coefficient for incident radiation in element i; μ_1—mass attenuation coefficient for incident radiation in a sample; μ_2—mass attenuation coefficient for fluorescence radiation in a sample; φ_1—incident angle; φ_2—take-off angle.

This formula is simplified; the full expression is described by Beckhoff et al. (2006). The data from Fig. 2a and b was evaluated using the fundamental parameter method, and the concentrations of iron and nickel were again normalized to 100%. As expected, the concentrations of iron, displayed in Fig. 3b, show lower fluctuations than in Fig. 3a. However, the artifact caused by surface roughness is still significant.

The aim of further investigations was to test new methods for reducing the surface effect. The first of these methods utilizes a geometry setup with a close arrangement of the incident and emergent radiation. Theoretically, the surface effects disappear altogether for geometry 90°/90°. However, this geometry is not attainable in practice due to the sizes and the shapes of the X-ray sources and detectors. The surface effect can be reduced to some